

## Kinetics of the Heterogeneous Reaction $\text{HNO}_3(\text{g}) + \text{NaBr}(\text{s}) \rightleftharpoons \text{HBr}(\text{g}) + \text{NaNO}_3(\text{s})$

Ming-Tsun Leu\*, Raimo S. Timonen, and Leon F. Keyser

Earth and Space Sciences Division, Jet Propulsion Laboratory, California Institute of Technology, Pasadena, CA 91109

### Abstract

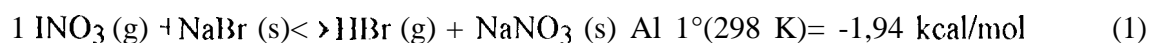
The kinetics of the heterogeneous reaction  $\text{HNO}_3(\text{g}) + \text{NaBr}(\text{s}) \rightleftharpoons \text{HBr}(\text{g}) + \text{NaNO}_3(\text{s})$  has been investigated at 296 K using a fast-flow reactor coupled to an electron-impact ionization mass spectrometer. The concentrations of  $\text{HNO}_3$  and  $\text{HBr}$  in the presence of salts were monitored mass spectrometrically and their decay rates were used to obtain uptake coefficients. The sizes of  $\text{NaBr}$  and  $\text{NaNO}_3$  granules were measured using an optical microscope and their specific surface areas were estimated by a well known relationship,  $S_g = 6/d\rho_t$ , where  $d$  is the average diameter of the granule and  $\rho_t$  is the true density of the  $\text{NaBr}$  or  $\text{NaNO}_3$  substrate. Our observations indicate that the uptake process comprises both physical adsorption and chemical reaction. The uptake coefficients for the forward and reverse processes, after accounting for internal surfaces by means of a mathematical model of surface reaction and pore diffusion, were found to be  $(2.8 \pm 0.5) \times 10^{-3}$  and  $(1.2 \pm 0.2) \times 10^{-2}$  at 296 K, respectively. The error limits represent for one standard deviation, precision only. The implications for atmospheric chemistry in the marine boundary layer and Arctic troposphere are discussed.

\* Author to whom correspondence should be addressed.

nabr1.doc (8-13-96)

## Introduction

The forward reaction (1 f) between gaseous  $\text{HNO}_3$  and solid  $\text{NaBr}$



is of interest for the following reasons. First, heterogeneous reactions involving  $\text{NaBr}$  have been suggested to play an important role in ozone depletion in the Arctic troposphere [1-3]. Recent field studies in the spring at Alert, Canada show that ground-level ozone concentrations decrease dramatically in a period of time ranging from a few hours to a few days [4-6]. The studies also demonstrate that there is a strong correlation between ozone destruction and filterable bromine (the sum of Br on particles and gaseous species, such as  $\text{HBr}$  efficiently collected by a combination Teflon/nylon filter). Also, both gaseous and particulate bromine compounds have been found in the marine boundary layer around the world [7-9]. Thus, bromine photochemistry, including some heterogeneous reactions, has been invoked to explain the ozone loss. Secondly, numerous studies of heterogeneous  $\text{NaCl}$  reactions have been documented in the literature [10-13]. These were motivated by the discovery of salt particles in the stratosphere after the El Chichon volcanic eruptions [14] and the subsequent measurement of the enhancement of hydrochloric acid [15-17]. Similarly, reactions on  $\text{NaCl}$  aerosols in the marine boundary layer have been used to explain measurements of  $\text{HCl}$  and  $\text{HNO}_3$  [18-20]. A study of bromine heterogeneous reactions is a useful extension of this work.

In a previous study of reaction (1 f), Fenter et al [12] used a low pressure Knudsen cell and obtained a value of  $\gamma(1f) = 0.028$  at room temperature. This value was based on only one experiment and was comparable to the reaction probabilities on other salts. Moreover, the result was not corrected for the effect of internal surface area of the  $\text{NaBr}$  substrate. To our knowledge, there is no previous study of the reverse reaction (1 r).

In this article we report experimental results for both reactions (1 f) and (1 r). By using a fast-flow reactor coupled to a differentially-pumped quadrupole mass

spectrometer, the kinetic mechanism was investigated. Moreover, a mathematical model of surface reaction and pore diffusion was used to obtain uptake coefficients in a manner similar to our previous studies on reactions of NaCl with ClONO<sub>2</sub>, HNO<sub>3</sub>, and N<sub>2</sub>O<sub>5</sub> [10,11]. The implication for atmospheric chemistry in the marine boundary layer and Arctic troposphere will be briefly discussed.

### Experimental Method

The uptake coefficient measurement was performed in a fast-flow reactor coupled to an electron-impact ionization mass spectrometer as shown in Figure 1 [10,11,21]. The flow reactor was made of borosilicate glass, and its dimensions were 20.0 cm in length and 1.8 cm inside diameter. The bottom of the reactor was recessed and flattened in order to hold the NaBr or NaNO<sub>3</sub> substrates in place. The depth of the recess was about 0.33 cm. Temperature was regulated by circulating cold methanol through a jacket surrounding the flow reactor and the temperature was measured by a thermocouple attached to the middle section. The pressure inside the reactor was monitored by a high-precision capacitance manometer which was located about 7 cm from the reactor at the downstream end. The measured pressure was corrected for the viscous pressure gradient between the measurement point and the midpoint of the reactor. The carrier gas, helium, was admitted to the reactor through a side-arm inlet. The gas-phase reactants, HNO<sub>3</sub> or HBr, were added through a sliding borosilicate injector. The average flow velocity in the flow-tube reactor was calculated to be between 1400 and 1800 cm/s. A large metal valve located at the downstream end of the reactor was used to regulate the flow velocity.

HNO<sub>3</sub> was prepared by reacting 112S04 (96 wt%) with reagent grade NaNO<sub>3</sub> (99%) in vacuum and the nitric acid vapor was collected in a Pyrex vessel at liquid nitrogen temperature. The HNO<sub>3</sub> thus prepared was further purified by vacuum distillation at 195 K. HBr about 1% was mixed with helium in a 5-l. glass vessel and its flow rate was measured by a mass flowmeter. HNO<sub>3</sub> and HBr were monitored by the mass spectrometer using  $m/e = 46$  and  $80$  AMU, respectively.

Two batches of NaBr were obtained from E. Merck Corp. The size and shape of the granules were examined by using an optical microscope. The typical shape was cubic, and the average sizes were found to be about 0.276 mm for batch 1 and 0.249 mm for batch 2, respectively. The specific surface area,  $S_g$ , can be calculated from the average crystal size by using [22]

$$S_g = 6/\rho_t d \quad (2)$$

where  $\rho_t$  is the true density of NaBr ( $3.204 \text{ g/cm}^3$ ) [23] and  $d$  is the granule size. One batch of  $\text{NaNO}_3$  was purchased from Fisher and its average size was about 0.190 mm. Another batch was supplied by J. T. Baker and the average size was smaller (0.145 mm). The true density of  $\text{NaNO}_3$  is  $2.261 \text{ g/cm}^3$  [23]. In typical experiments these substrates were placed in the reactor and then were baked in vacuum for at least 4 hours. However, in some experiments they were not heated in order to test the effect of surface moisture on reactivity. The results will be discussed later.

The procedure used in determining the reaction probability is similar to that in our previous studies [10,11] and will be briefly discussed as follows. The loss rates of  $\text{HNO}_3$  and  $\text{HBr}$  were measured as a function of inlet position,  $z$ . The reaction time was calculated by using  $t = z/v$  where  $v$  is the average flow velocity. In each experiment we calculated the cross sectional area of the reactor and then the flow velocity. The first-order rate constant,  $k_s$ , was calculated from the slope of a linear least-squares fit to the experimental data. The axial gas-phase diffusion correction for  $k_s$  was made by using the following equation [24]

$$k_g = k_s (1 - k_s D/v^2) \quad (3)$$

The diffusion coefficients of HNO<sub>3</sub> and HBr in helium were estimated to be  $D = 495$  Torr cm<sup>2</sup>s<sup>-1</sup> and  $440$  Torr cm<sup>2</sup> s<sup>-1</sup> at 296 K, respectively [25]. The rate corrected for gas-phase diffusion is designated as  $k_g$ .

For radial gas-phase diffusion, it is more difficult to estimate the correction to  $k_s$  because the reactor is no longer a fully symmetric cylindrical tube. If we use the full reactor radius of 0.9 cm in the calculation, the correction is relatively small, less than 10%. Since this correction is not precise, we neglected it in the data analysis.

On the basis of the geometric area ( $S$ ) which was used to hold the NaBr or NaNO<sub>3</sub> substrates and the volume ( $V$ ) of the reactor, the reaction probability,  $\gamma_g$ , was then calculated by using the following equation [26]

$$\gamma_g = 4k_g V / \bar{w} S \quad (4)$$

where  $\bar{w}$  is the average molecular velocity for HNO<sub>3</sub> or HBr at 296 K. Note that this equation is valid for  $\gamma_g < 0.1$  only, which holds for the present experiments.

To account for the surfaces of the salt granules beneath the top layer, we used an analysis recently developed and successfully applied to heterogeneous reactions on porous ice films [27]. We model the NaBr or NaNO<sub>3</sub> substrates as hexagonal close-packed (HCP) spherical granules stacked in layers. For this model, the following equation holds

$$\gamma_t = \gamma_g \pi^{-1/2} \{1 + \eta[2(N_L - 1) + (3/2)^{1/2}]\}^{-1} \quad (5)$$

where  $\gamma_t$  is the true reaction probability for reactions (1) and (2), and  $N_L$  is the number of granule layers or the ratio of the thickness of the salt substrates to the average granule size. In eq 5,  $\eta$  is the effectiveness factor, which is the fraction of the NaBr or NaNO<sub>3</sub> surface that participates in the reaction. This factor is determined by the relative rates of pore diffusion to surface reaction and is given by

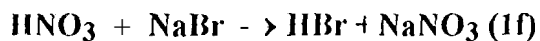
$$\eta = \phi^{-1} \tanh \phi \quad (6)$$

$$\phi = (h_i/d)[3\rho_b/2(\rho_t - \rho_b)](3\tau\gamma_t)^{1/2} \quad (7)$$

where  $h_i$  is the internal thickness of the salt substrates,  $d$  is the average size of granules,  $\rho_b$  is the bulk density,  $\rho_t$  is the true density and  $\tau$  is a tortuosity factor. Typically, this factor is between 1.7 and 4 [28]. In our data analysis, we used a value of 2. This type of calculation has been successfully used in previous publications [10,11].

In general, the magnitude of the corrections that convert  $\gamma_g$  to  $\gamma_t$  is less than a factor of 3 for  $\gamma_t > 0.1$ . However, for  $\gamma_t < 0.1$ , the correction factors become much larger [26,27]. The possible uncertainties in the correction factors can be estimated by assessing the expected errors introduced by uncertainties in  $N_I$ ,  $\tau$ , and the type of packing (bulk density). For an uncertainty in  $N_I$  of  $\pm 2$  within the range used, the errors in the correction factors are less than 15%. For  $\tau = 2$  or 3 [28], the error in the correction factors is less than  $\pm 20\%$ . For layer packing between simple cubic packing (SCP) and HCP, the correction factor error ranges over  $\pm 25\%$ . Including the errors ( $\pm 15-25\%$ ) associated with the measurements of temperature, total pressure, flow rates, external gas-phase diffusion correction, we estimate that the systematic error is about a factor of 2.

## Results and Discussion



The uptake of  $\text{HNO}_3$  in the presence of  $\text{NaBr}$  is shown in Figure 2. The experimental conditions were  $p(\text{HNO}_3) = 6.7 \times 10^{-7}$  Torr,  $m(\text{NaBr}) = 28$  g,  $p = 0.462$  Torr, and  $v = 1716$  cm/s. initially the sliding injector was positioned downstream of the

NaBr substrate. After about 4 minutes, the reaction was started by moving the injector upstream of the substrate. The uptake or loss of  $\text{HNO}_3$  coincided with the appearance of  $\text{HBr}$  from the NaBr surface. The gradual rise in the  $\text{HNO}_3$  signal was an indication of surface deactivation. At about 30 minutes the injector was moved downstream and the  $\text{HBr}$  signal dropped to near zero while the  $\text{HNO}_3$  signal was higher than the initial value. This sequence was repeated one more time at about 36 and 60 minutes. After calibration of  $\text{HNO}_3$  and  $\text{HBr}$  signals, the uptake of  $\text{HNO}_3$  was found to be about  $1.8 \times 10^{17}$  molecules and the yield of  $\text{HBr}$  was found to be about  $6.1 \times 10^{16}$  molecules. These observations suggest that the yield of  $\text{HBr}$  is about 34% of the uptake of  $\text{HNO}_3$ . Furthermore, the observation of an increase in the  $\text{HNO}_3$  signal when the injector was moved downstream is evidence that some of the  $\text{HNO}_3$  may also be physically adsorbed on the NaBr surface. In a separate experiment we measured the physical uptake of  $\text{HNO}_3$  on the  $\text{NaNO}_3$  substrates and we did not find any reaction products formed. Similarly, some of the  $\text{HBr}$  may also stay on the surface of salts. This finding is consistent with the observation of the uptake of  $\text{HCl}$  on  $\text{NaCl}$  powders reported by Fenter et al, [ 12] 't'bus, the uptake of  $\text{HNO}_3$  on the surface of NaBr comprises two components: physical uptake and reactive uptake.

The uptake coefficients of  $\text{HNO}_3$  on NaBr were measured by monitoring  $\text{HNO}_3$  signals while moving the injector from downstream to upstream and by calculating the decay rate of  $\text{HNO}_3$ . The procedure has been discussed in the preceding section. Under plug-flow conditions, the decay of  $\text{HNO}_3$  is given by the equation

$$\ln[S(z)] = -k_s(z/v) + \ln[S(0)] \quad (8)$$

Typical data of the  $\text{HNO}_3$  loss as a function of injector position are shown in Figure 3. The experimental conditions were  $p(\text{HNO}_3) = 7.0 \times 10^{-7}$  Torr,  $m(\text{NaBr}) = 28$  g,  $v = 1611$  ends, and  $p = 0.372$  Torr. The salt was baked for a few hours at a temperature of 443 K. We repeated the same procedure several times and obtained a value of  $\gamma_g(1f) = 0.022$  in this experiment. The total exposure time was always less than 10-20 seconds in order to prevent any significant surface deactivation. After correcting for the internal surface area, we found  $\gamma_t(1f) = 0.0019$ . Moreover, we have used two batches of samples supplied from Merck (see Experimental Section) and performed the experiments by using the dry salts or unbaked samples in order to check the effect of moisture on the uptake. The results are summarized in Table 1. The data obtained by using the unbaked salts appears to be about 20% greater than those for baked salts. But the difference is within the quoted uncertainties and is considered to be insignificant. The average value of these measurements is  $\gamma_t(1f) = (2.8 \pm 0.5) \times 10^{-3}$  at 296 K. The error limit represents for one standard deviation, precision only. It is also noted that on the basis of the external geometric area of the NaBr substrate,  $\gamma_g(1f)$  is 0.03, about a factor of 10 greater than  $\gamma_t(1f)$  due to the effect of the internal surface area,



We also studied the uptake of  $\text{HBr}$  in the presence of  $\text{NaNO}_3(1r)$  by using a procedure similar to that used for the reaction (1f). One example of the experiment is shown in Figure 4. The uptake of  $\text{HBr}$  and the yield of  $\text{HNO}_3$  decreased during the exposure of  $\text{NaNO}_3$  suggesting that some deactivation of the surface may have occurred. The yield of  $\text{HNO}_3$  was only about 10-30 % of the  $\text{HBr}$  uptake. This implies that both physical and reactive uptake are occurring. Desorption of  $\text{HBr}$  was not observed during the experiment on the basis of the observation that the  $\text{HBr}$  signal was nearly constant



when the injector was moved downstream (see Figure 4). This implies that IIBr is more strongly adsorbed on NaNO<sub>3</sub> than HNO<sub>3</sub> is on NaBr (see Figure 2).

The uptake coefficient was also measured by placing about 19 g of NaNO<sub>3</sub> inside the flow reactor and by monitoring the decay rate of IIBr while moving the injector from downstream to upstream and then moving the injector from upstream to downstream. The data are shown in Figure 5. The experimental conditions were  $p(\text{IIBr}) = 6.5 \times 10^{-7}$  Torr,  $v = 1737$  cm/s, and  $p = 0.470$  Torr. We repeated the same procedure and obtained a consistent value  $\gamma_t(1r) = 0.014$  in this experiment. Again, we used two batches of samples, one supplied from Fisher Co. and another from Baker Co. The results are summarized in Table 2. It appears that there is no difference between the data for dry salts and unbaked salts. The average value of these measurements is  $\gamma_t(1r) = 0.012 \pm 0.002$  at 296 K. The error limit represents for one standard deviation, precision only. It appears that the rate for the forward reaction (1f) is about a factor of 4 smaller than that for the reverse reaction (1r).

The change in entropy for reaction(1) can be estimated to be  $\Delta S^\circ(298 \text{ K}) = -9.48$  cal mol<sup>-1</sup> K<sup>-1</sup> on the basis of the ratio  $\gamma_t(1f)/\gamma_t(1r)$  measured in this experiment. The result is in good agreement with the value of  $\Delta S^\circ(298 \text{ K}) = -9.08$  cal mol<sup>-1</sup> K<sup>-1</sup> obtained using thermodynamic data [23]. This suggests that our measurements of uptake coefficients for reaction (1) are reasonable.

In a previous investigation by Fenter et al. [12] using a Knudsen cell reactor, they obtained a value of 0.028 for the uptake of HNO<sub>3</sub> on NaBr. It should be noted that their value is not corrected for the porous nature of salts. On the basis of the external geometric area of salt substrates, our data of  $\gamma_g = 0.03$  is in excellent agreement with their data of 0.028, despite the difference in experimental methods used.

It is also interesting to note that the uptake of  $\text{HNO}_3$  on  $\text{NaCl}$  ( $\gamma_t = 0.013$ ) measured previously in our laboratory [ 11 ] is about a factor of 5 greater than the uptake of  $\text{HNO}_3$  on  $\text{NaBr}$  reported in this work.

The atmospheric significance of reaction (1) clearly depends on the rate coefficients and also concentrations of gas species and salt particles. In this article we have measured rate coefficients for (1) at ambient temperature. However, the concentrations of  $\text{HNO}_3$ ,  $\text{HBr}$ ,  $\text{NaBr(s)}$ , and  $\text{NaNO}_3(\text{s})$  vary drastically in the atmosphere. We will discuss this matter separately for two regions of the atmosphere.

*Troposphere.* In the marine boundary layer the gas-phase nitric acid mixing ratio is about 1 ppbv [18,19]. It is interesting to investigate the uptake of nitric acid by sea salt particles. Because concentrations of bromides are about two orders of magnitude smaller than chlorides in sea-salt particles [7-9] and the uptake coefficient for (1) is about a factor of 5 smaller than the uptake of  $\text{HNO}_3$  by  $\text{NaCl}$ , we conclude that  $\text{HNO}_3$  predominantly reacts with  $\text{NaCl}$  rather than  $\text{NaBr}$  in the marine boundary layer.

In the arctic troposphere there is a strong correlation between ozone loss and filtered-bromine (i.e., bromine compounds that can be collected on cellulose filters or Teflon/nylon filters). It is possible that  $\text{NaBr}$  may be present, in addition to  $\text{HBr}$  or  $\text{BrO}$ , in the measurement of filtered bromine. Hence, it is likely that reaction (1) may play a role in the Arctic ozone loss.

*Stratosphere.* As discussed in the introduction section, chloride particles were observed in the lower stratosphere a few months after the eruption of El Chichon by Woods et al. [14] and a significant enhancement of hydrogen chloride was measured using infrared spectrometry [15]. In our previous articles [10,11] we have suggested that heterogeneous reactions on  $\text{NaCl}$  particles may be responsible for this enhancement. However, it is possible that small amounts of bromides may accompany the chlorides in volcanic emissions. If  $\text{NaBr}$  were also injected from El Chichon, reaction (1) could transform the solid bromide salts into hydrogen bromide. To our knowledge, there was no such measurement of  $\text{HBr}$  column density made in 1982. The observation would be very

difficult because the background concentration is as low as 1-2 pptv [29]. Therefore, it is not possible to conclude that reaction (1f) played any role in stratospheric chemistry after the eruption of El Chichon.

## Conclusions

In this paper we have reported the kinetic measurements for the forward and reverse processes of reaction (1). The uptake coefficients for  $k(1f) = (2.8 \pm 0.5) \times 10^{-3}$  and  $k(1r) = (1.2 \pm 0.2) \times 10^{-2}$  were obtained at 296 K, respectively. These uptake processes were found to comprise both physical adsorption and heterogeneous reaction.

**Acknowledgment.** The research described in this article was performed at the Jet Propulsion Laboratory, California Institute of Technology, under contract with the National Aeronautics and Space Administration. R. S. T. gratefully acknowledges the financial support from Maj and Tor Nessling Foundation.

## References and Notes

- (1) Finlayson-Pitts, B. J.; Livingston, F. E.; Berko, H. N. *Nature* 1990, 347, 622.
- (2) Berko, H. N.; McCaslin, P. C.; Finlayson-Pitts, B. J. *J. Phys. Chem.* 1991, 95, 6951.
- (3) Fan, S.-M.; Jacob, D. J. *Nature* 1992, 359, 522.
- (4) Bottenheim, J. W. et al. *J. Geophys. Res.* 1990, 95, 18555.
- (5) Oltmans, S. J. et al. *Atmos. Environ.* 1989, 23, 2431.
- (6) McConnell, J. C. et al. *Nature*, 1992, 355, 150.
- (7) Moyers, J. I.; Duce, R. A. *J. Geophys. Res.* 1972, 77, 5330.
- (8) Duce, R. A.; Zoller, W. H.; Moyers, J. I. *J. Geophys. Res.* 1973, 78, 7802.
- (9) Sturges, W. T.; Barrie, L. A. *Atmos. Environ.* 1988, 22, 1179.
- (10) Timonen, R. S.; Chu, L. T.; Leu, M.-T.; Keyser, L. F. *J. Phys. Chem.* 1994, 98, 9509.
- (11) Leu, M.-T.; Timonen, R. S.; Keyser, L. F.; Yung, Y. L. *J. Phys. Chem.* 1995, 99, 13203.
- (12) Fenter, F. F.; Caloz, F.; Rossi, M. J. *J. Phys. Chem.* 1994, 98, 9801.
- (13) Laux, J. M.; Hemminger, J. C.; Finlayson-Pitts, B. J. *Geophys. Res. Lett.* 1994, 21, 162.
- (14) Woods, D. C.; Chuan, R. L.; Rose, W. L. *Science* 1985, 230, 170.
- (15) Mankin, W. G.; Coffey, M. T. *Science* 1984, 226, 170.
- (16) Michelangeli, D. G.; Allen, M.; Yung, Y. L. *Geophys. Res. Lett.* 1991, 18, 673.
- (17) Michelangeli, D. G.; Allen, M.; Yung, Y. L. *J. Geophys. Res.* 1989, 94, 18429.
- (18) Solomon, P. A.; Salmon, L. G.; Fall, T.; Cass, G. R. *Environ. Sci. Technol.* 1992, 26, 1894.
- (19) Eldering, A.; Solomon, P. A.; Salmon, L. G.; Fall, T.; Cass, G. R. *Atmos. Environ.* 1991, 25, 2091.
- (20) Pszenny, A. A. P. et al. *Geophys. Res. Lett.* 1993, 20, 699.
- (21) Chu, L. T.; Leu, M.-T.; Keyser, L. F. *J. Phys. Chem.* 1993, 97, 7779.

- (22) Gregg, S. J.; Sing, K. S. W. *Adsorption, Surface Area and Porosity*, Academic Press: New York, 1982.
- (23) Weast, R. C. *Handbook of Chemistry and Physics*, 65th ed.; CRC Press: Boca Raton, FL, 1984.
- (24) Kaufman, F. *Prog. React. Kinet.* 1961, 1, 1.
- (25) Marreo, P. R.; Mason, E. A. *J. Phys. Chem. Ref. Data* 1972, 1, 3.
- (26) Keyser, L. F.; Moore, S. B.; Leu, M.-J. *J. Phys. Chem.* 1991, 95, 5496.
- (27) Keyser, L. F.; Leu, M.-J.; Moore, S. B. *J. Phys. Chem.* 1993, 97, 2800.
- (28) Satterfield, C. N. *Heterogeneous Catalysis in Industrial Practice*. 2nd ed.; McGraw-Hill, Inc.: New York, 1991.
- (29) Johnson, D. G.; Traub, W. A.; Chance, K. V.; Jucks, K. W. *Geophys. Res. Lett.* 1995, 22, 1373.

**Table 1.** Summary of the reaction probability measurements for the reaction  $\text{HNO}_3(\text{g}) + \text{NaI}(\text{s}) \rightarrow \text{HBr}(\text{g}) + \text{NaNO}_3(\text{s})$  at 296 K. The errors indicate one standard deviation.

NaBr substrate	no. of experiments	$\gamma_t (10^{-3})$
Baked (Merck 1)	43	2,5 ± 10.6
Baked (Merck 2)	12	2.6 ± 0.7
Unbaked (Merck 1)	42	3.0 ± 0.7
Unbaked (Merck 2)	8	3.1 ± 0.2
	Average Value	2,8 ± 0.5

**Table 2.** Summary of the reaction probability measurements for the reaction  $1 \text{ HBr(g)} + 1 \text{ NaNO}_3(\text{s}) \rightarrow \text{HNO}_3(\text{g}) + \text{NaBr}(\text{s})$  at 296K. The errors indicate one standard deviation.

$\text{NaNO}_3$ substrate	no. of experiments	$\gamma_t (10^{-2})$
Baked (Fisher)	10	$1.1 \pm 0.2$
Baked (Baker)	59	$1.2 \pm 0.3$
Unbaked (Baker)	20	$1.2 \pm 0.2$
	Average Value	$1.2 \pm 0.2$

## Figure Captions

Figure 1. Schematic diagram of a fast-flow reactor coupled to an elect ion-impact ionization mass spectrometer. The bottom of the reactor was recessed and flattened for the preparation of salt substrates. See text for details.

Figure 2. Uptake of  $\text{HNO}_3$  by  $\text{NaBr}$  at 296 K. Both the  $\text{HNO}_3$  loss (upper curve) and  $\text{HBr}$  growth (lower curve) were monitored.

Figure 3. Loss of  $\text{HNO}_3$  signals as a function of injector position at 296 K. Closed square arc for data obtained when the injector was moved from downstream to upstream, Closed circles arc for data obtained when the injector was moved from upstream to downstream.

Figure 4. Uptake of  $\text{HBr}$  by  $\text{NaNO}_3$  at 296 K. Both the  $\text{HBr}$  loss (upper curve) and  $\text{HNO}_3$  growth (lower curve) were monitored.

Figure 5. Loss of  $\text{HBr}$  signals as a function of injector position at 296 K, Closed squares are for data obtained when the injector was moved from downstream to upstream. Closed circles arc for data obtained when the injector was moved from upstream to downstream.



# NEUTRAL FLOW REACTOR

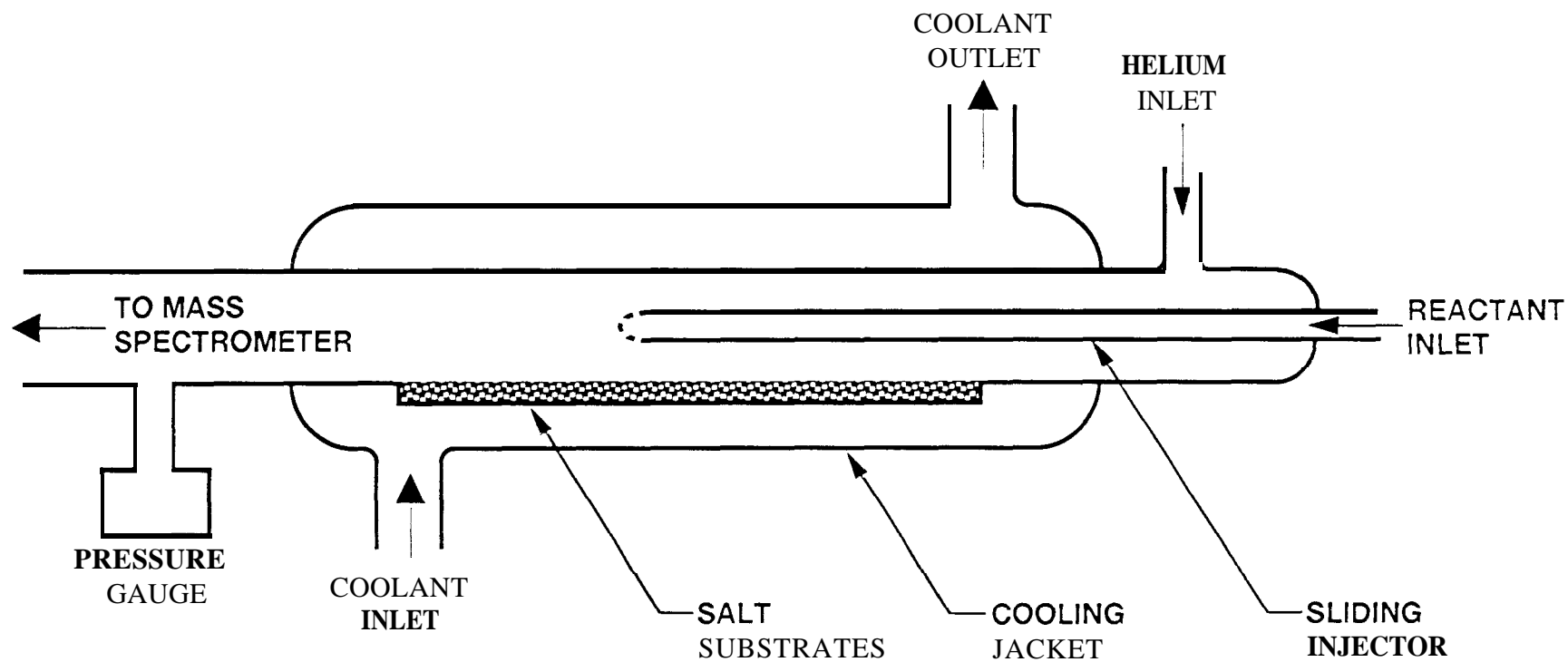


Fig 1

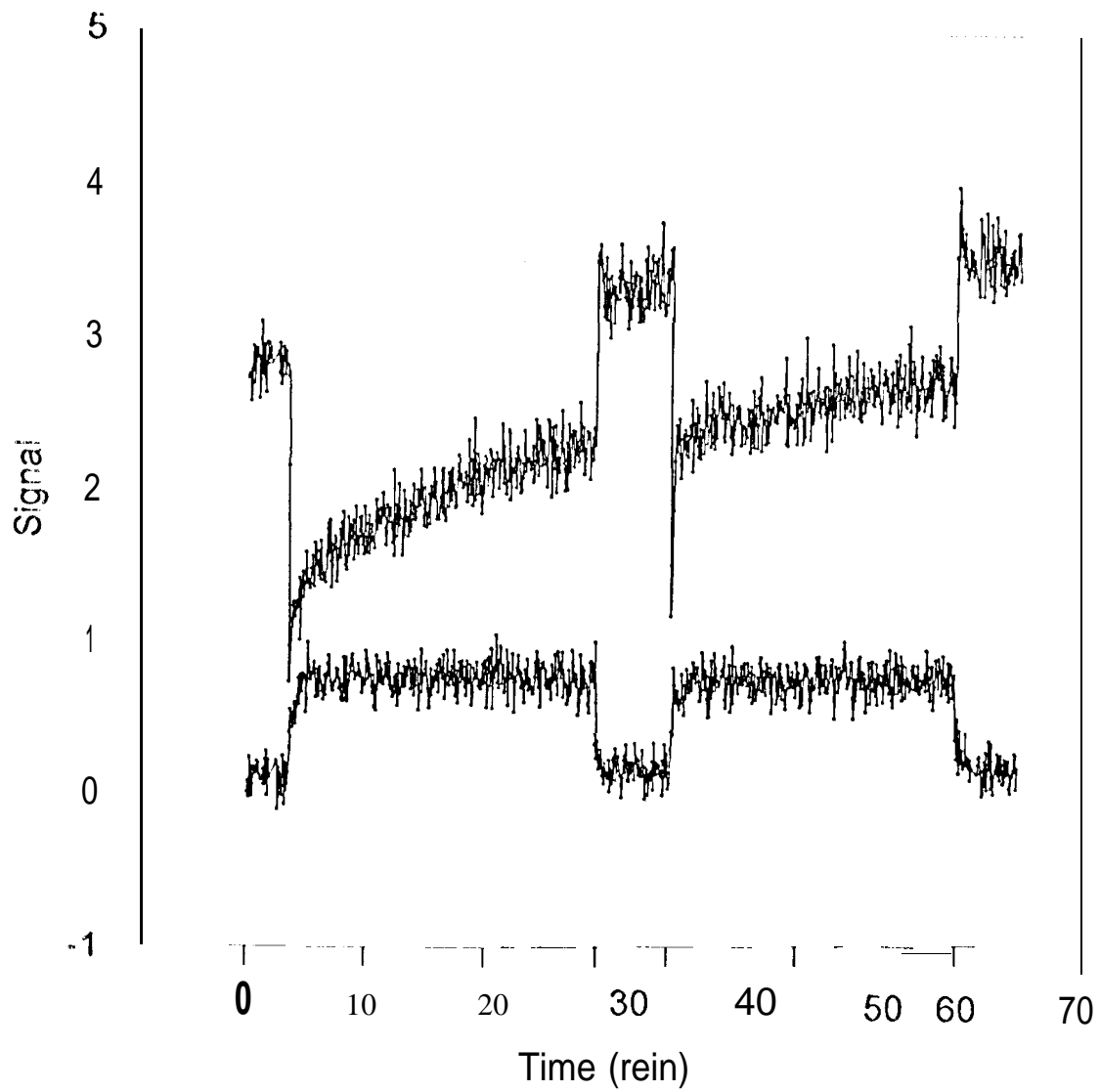
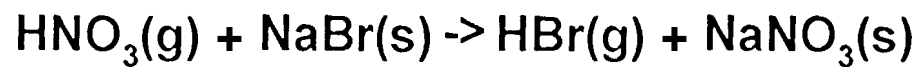


Fig. 2

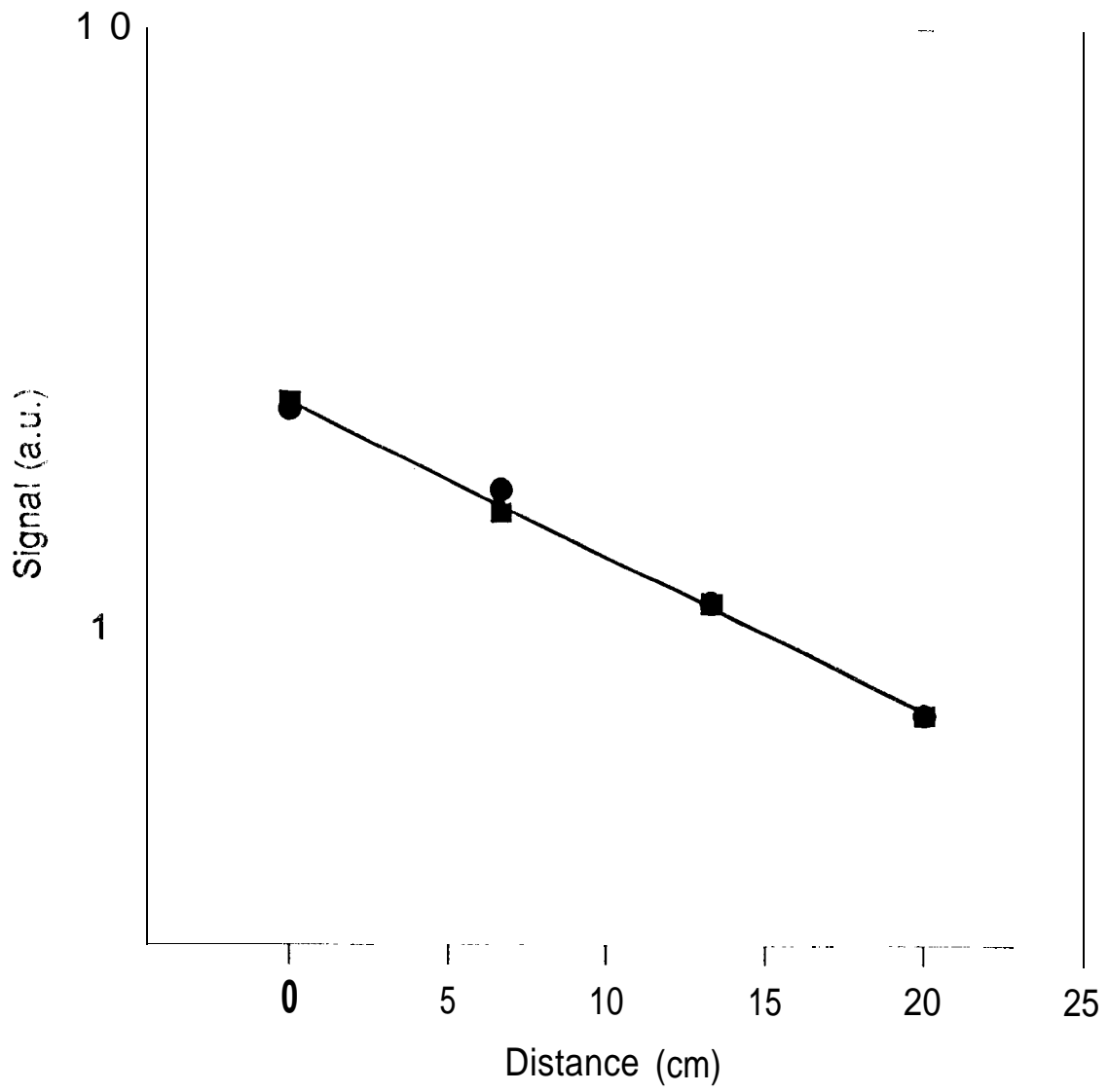
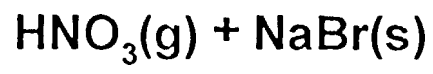


Fig. 3

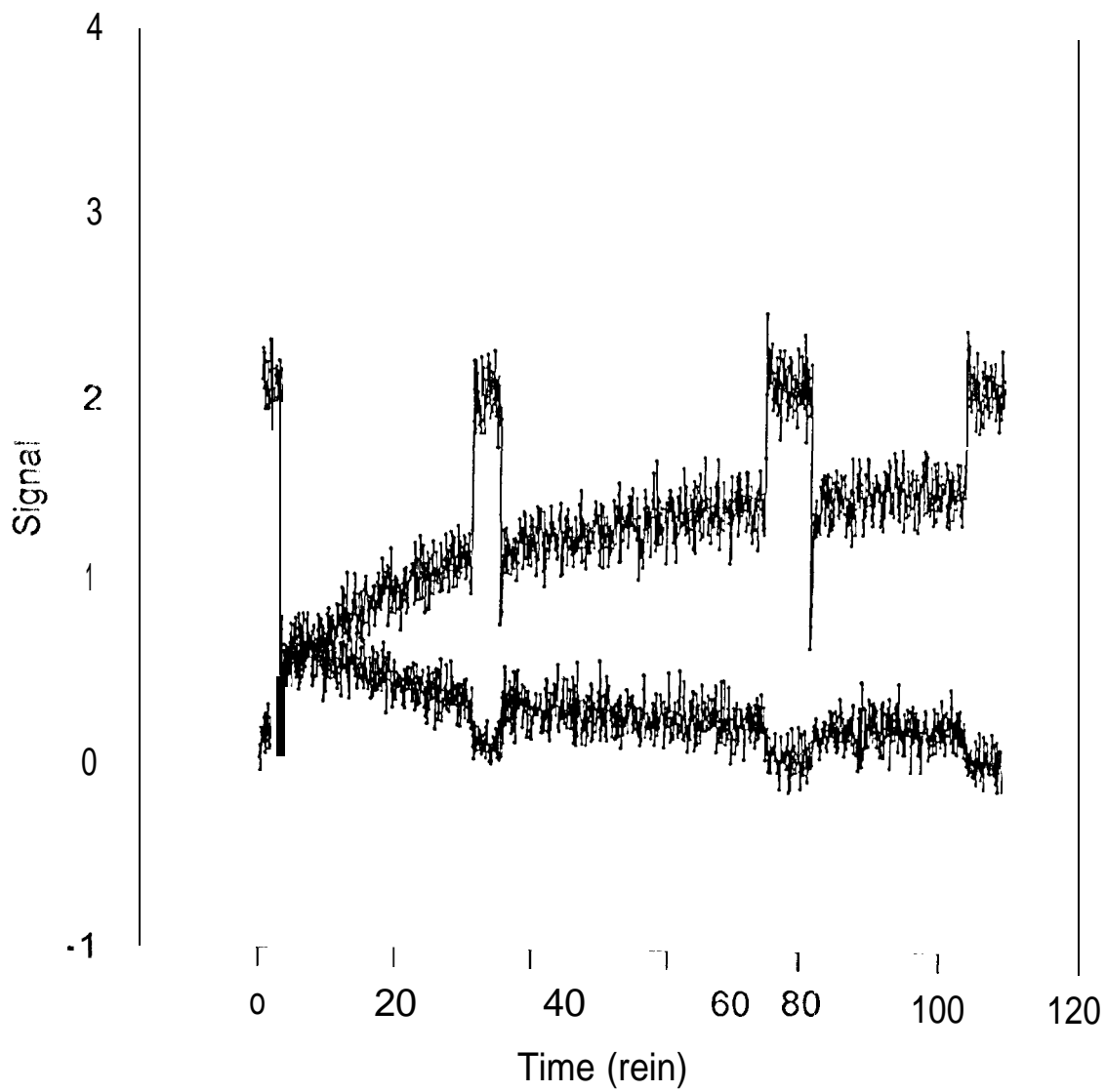


Fig. 4

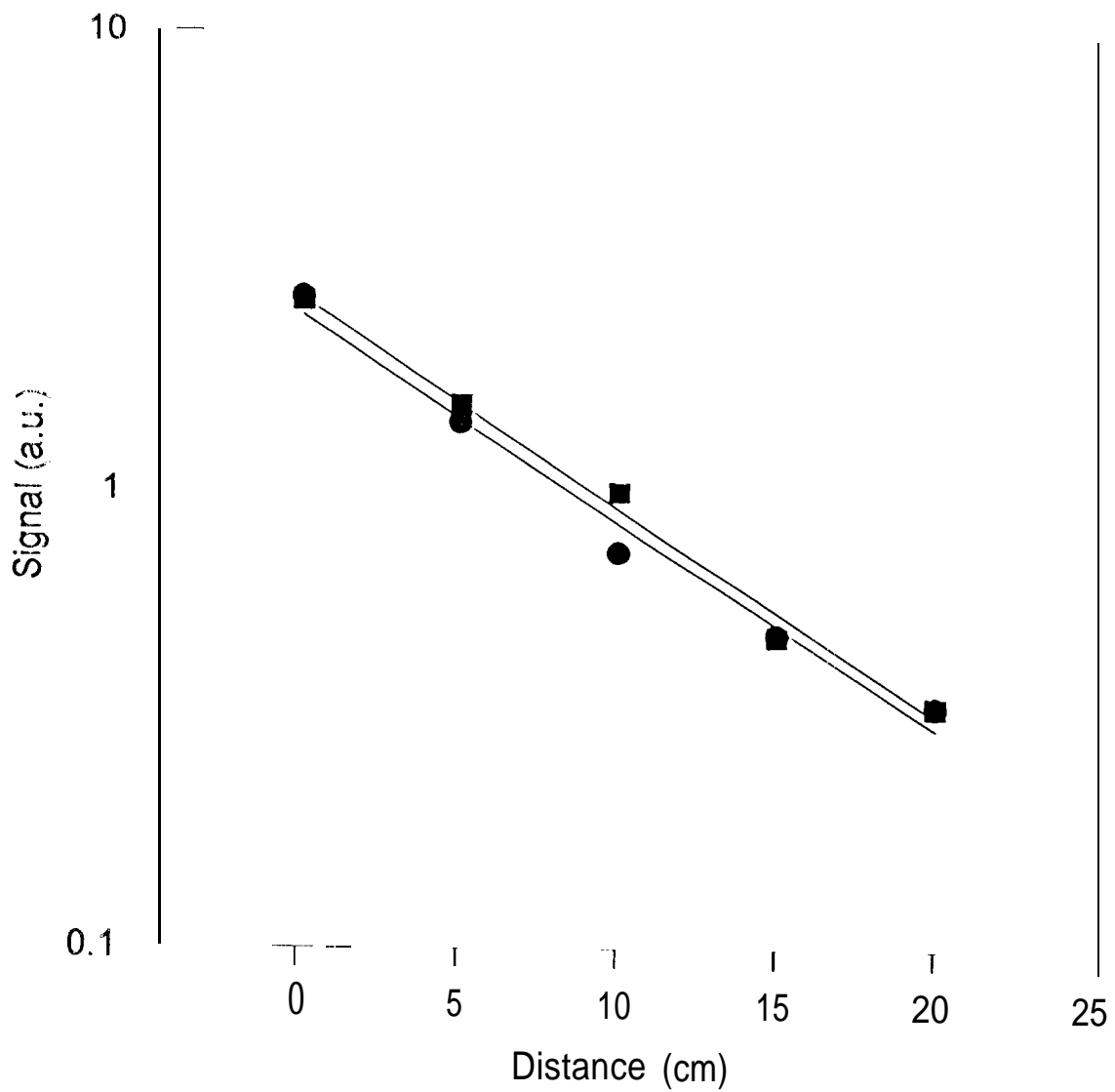
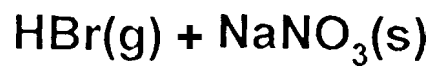


Fig. 5